

## ORIGINAL ARTICLE

# Lack of serotonin<sub>1B</sub> receptor expression leads to age-related motor dysfunction, early onset of brain molecular aging and reduced longevity

E Sibille<sup>1,2</sup>, J Su<sup>1</sup>, S Leman<sup>3</sup>, AM Le Guisquet<sup>3</sup>, Y Ibarguen-Vargas<sup>3</sup>, J Joeyen-Waldorf<sup>1</sup>, C Glorioso<sup>2</sup>, GC Tseng<sup>4</sup>, M Pezzone<sup>5</sup>, R Hen<sup>6</sup> and C Belzung<sup>3</sup>

<sup>1</sup>Department of Psychiatry, University of Pittsburgh, Pittsburgh, PA, USA; <sup>2</sup>Center for Neuroscience, University of Pittsburgh, Pittsburgh, PA, USA; <sup>3</sup>EA3248 Psychobiologie des émotions, Faculté des Sciences et Techniques, Université François Rabelais, Tours, France; <sup>4</sup>Department of Biostatistics, University of Pittsburgh, Pittsburgh, PA, USA; <sup>5</sup>Department of Medicine, University of Pittsburgh, Pittsburgh, PA, USA and <sup>6</sup>Center for Neurobiology and Behavior, Columbia University, New York, NY, USA

Normal aging of the brain differs from pathological conditions and is associated with increased risk for psychiatric and neurological disorders. In addition to its role in the etiology and treatment of mood disorders, altered serotonin (5-HT) signaling is considered a contributing factor to aging; however, no causative role has been identified in aging. We hypothesized that a deregulation of the 5-HT system would reveal its contribution to age-related processes and investigated behavioral and molecular changes throughout adult life in mice lacking the regulatory presynaptic 5-HT<sub>1B</sub> receptor (5-HT<sub>1B</sub>R), a candidate gene for 5-HT-mediated age-related functions. We show that the lack of 5-HT<sub>1B</sub>R (*Htr1b*<sup>KO</sup> mice) induced an early age-related motor decline and resulted in decreased longevity. Analysis of life-long transcriptome changes revealed an early and global shift of the gene expression signature of aging in the brain of *Htr1b*<sup>KO</sup> mice. Moreover, molecular changes reached an apparent maximum effect at 18-months in *Htr1b*<sup>KO</sup> mice, corresponding to the onset of early death in that group. A comparative analysis with our previous characterization of aging in the human brain revealed a phylogenetic conservation of age-effect from mice to humans, and confirmed the early onset of molecular aging in *Htr1b*<sup>KO</sup> mice. Potential mechanisms appear independent of known central mechanisms (Bdnf, inflammation), but may include interactions with previously identified age-related systems (IGF-1, sirtuins). In summary, our findings suggest that the onset of age-related events can be influenced by altered 5-HT function, thus identifying 5-HT as a modulator of brain aging, and suggesting age-related consequences to chronic manipulation of 5-HT.

*Molecular Psychiatry* (2007) 12, 1042–1056; doi:10.1038/sj.mp.4001990; published online 10 April 2007

**Keywords:** serotonin; aging; longevity; cortex; Bdnf; sirtuin

## Introduction

Aging leads to morphological<sup>1–5</sup> and functional<sup>6–9</sup> changes in the brain and is associated with increased risk for psychiatric and neurological disorders.<sup>10–13</sup> However, the mechanisms underlying normal aging of the brain likely differ from those associated with neurodegenerative and pathological conditions and are still poorly understood.<sup>14</sup> Several lines of evi-

dence suggest a role for 5-HT during aging, including structural and functional age-related changes in the 5-HT system in rodents<sup>15–17</sup> and in humans, as documented by post-mortem receptor binding studies,<sup>18–20</sup> RNA level studies,<sup>21</sup> *in vivo* imaging studies<sup>22</sup> and neuroendocrine challenges.<sup>10</sup> Depending on the brain region investigated, the 5-HT modulation of cerebral glucose metabolism increases or decreases during normal aging, suggesting a deregulated control of 5-HT<sup>23</sup> (see also<sup>24</sup>). The mechanisms for age-related changes in 5-HT function are not known and may include gene variants, pharmacological manipulation in adult/old population or late-onset functional declines. Based on converging roles in energy metabolism, cellular signaling pathways and synaptic plasticity, interactions between 5-HT, neurotrophic function (brain-derived neurotrophic factor, Bdnf) and insulin-like growth factor (IGF) have been

Correspondence: Dr E Sibille, Department of Psychiatry, University of Pittsburgh, 3811 O'Hara Street, BST W1643, Pittsburgh, PA 15213, USA.

E-mail: sibilleel@upmc.edu or

Professor C Belzung, EA3248 Psychobiologie des émotions, Université François Rabelais de Tours, Parc de Granmont, Tours 37200, France.

E-mail: catherine.belzung@univ-tours.fr

Received 30 October 2006; revised 18 January 2007; accepted 8 February 2007; published online 10 April 2007

proposed as potential determinants of homeostasis and health during aging.<sup>25</sup> Therefore, due to the critical role of 5-HT in mood regulation, age-related changes in 5-HT function are considered a risk factor for developing mood disorders in older subjects.<sup>12</sup>

A candidate gene for deregulated 5-HT control in aging is the 5HT<sub>1B</sub> receptor (5HT<sub>1BR</sub>).<sup>26</sup> 5HT<sub>1BR</sub> is the predominant presynaptic autoreceptor modulating 5-HT release in the brain.<sup>27</sup> Decrease in 5HT<sub>1BR</sub> function, and not in its somatodendritic counterpart (5HT<sub>1AR</sub>), has been reported in aged rodents,<sup>26</sup> consistently with the role of this receptor subtype in motor function<sup>28</sup> and with the well-characterized decline in motor function during aging. As aging can be viewed as the accumulation of a variety of events that together create a chronic challenge to the brain, and since 5-HT is a key factor for adaptation to stress,<sup>29</sup> we hypothesized that a central deregulation of the 5-HT system in *Htr1b*<sup>KO</sup> mice would affect the brain response to this challenge and reveal the contribution of 5-HT to age-related processes. Accordingly, inactivation of 5HT<sub>1BR</sub> in *Htr1b*<sup>KO</sup> mice<sup>30</sup> results in mostly normal baseline, but altered 5-HT kinetics upon recruitment of the 5-HT system (i.e. increased release and higher synaptic levels), as revealed by pharmacological challenges and microdialysis studies.<sup>27,31,32</sup> Here we addressed the issue of causality versus correlation between 5-HT and aging, by investigating age-related behavioral and molecular changes as a result of the disruption of serotonin signaling through the 5HT<sub>1BR</sub> in *Htr1b*<sup>KO</sup> mice. We now show that the lack of 5HT<sub>1BR</sub>-mediated signaling induced both an early age-related motor decline and a global early shift of the characteristic gene expression signature of aging in the brain, ultimately resulting in decreased longevity, thus identifying 5-HT as a modulator of brain aging.

## Materials and methods

### Animals

All animals were raised under standard conditions: temperature 21 ± 2°C, controlled humidity 20–25%, 12:12 photoperiod with lights on at 20:00 to test animals during their scotophase. Food and water were available *ad libitum*. Weaning took place at 21 ± 1 days. At this age, animals were ear-punched and genotyped. Littermate wild-type (WT) and *Htr1b*<sup>KO</sup> mice were used for all behavior and microarray experiments, with the exception of animals used for the 3-month time point microarray analysis and for the serum-level measurements. These latter groups were no more than two generations away from heterozygous breeding. To avoid putative confounding effects of the previously reported increased aggressiveness of *Htr1b*<sup>KO</sup> mice,<sup>30</sup> WT and knockout (KO) mice were housed under reduced cage density, resulting in normal or low intra-cage aggression in both experimental groups, as revealed by the absence of bite marks or wounds. All experiments were conducted in accordance with the European Commu-

nities Council Directive of 24 November 1986 (86/609/EEC) and with the University of Pittsburgh Animal Care and Use Committee.

### Behavior

Separate groups of mice were tested at the age of 2, 6, 12 and 18 months, although all animals were generated and born approximately at the same time. This means that all animals were submitted to a battery of tests only once, according to the following schedule: open field, elevated-plus maze, rotarod and coat hanger tests. At least 1 week separated two different tests.

**Open field.** The apparatus consisted of a gray polyvinyl chloride circular open field, 40 cm in diameter and 30 cm high. The floor was divided into six peripheral and one circular central sectors, all of the same area (180 cm<sup>2</sup>) and covered by a white sheet of paper, which was changed after each mouse. A black–white stripped pattern, 30 × 20 cm, was present on the wall and provided a local cue. The device was lit by a red bulb placed 80 cm above the floor of the open field. Each mouse was introduced in the center of the open field and recorded for a period of 5 min. Numbers of peripheral and central sector crossings (total locomotion) and of rearing were recorded.

**Elevated plus maze.** The apparatus consists on two open and two closed 40 × 10 cm arms, located 40 cm above the floor. Mice were placed in the center and the time and number of entries in the closed and open arms were recorded for 5 min.

**Rotarod.** The apparatus consisted of a rotating horizontal rod located 25 cm above the floor. A fixed and relatively slow rotating speed was chosen (10 revolution per minute) to increase the sensitivity of this assay at older ages. One block of 10 trials was applied with an inter-trial interval of 10 min. The latency before falling was recorded with a cut-off point of 60 s.

**Coat hanger.** The triangular-shaped apparatus consisted of a horizontal steel wire (diameter: 2 mm, length: 41 cm) flanked at each end by two sidebars (length: 19 cm; inclination: 35° from the horizontal axis).<sup>33</sup> The horizontal bar was placed at a 45 cm height from the floor. The mice were placed upside-down in the middle of the horizontal wire and released only after gripping with all four paws. Latency before falling was recorded. A trial ended when the mice fell or reached the top of the apparatus, from which it was retrieved and the maximal score of 1 min given for latencies before falling. A block of five consecutive trials was applied with a 15-min inter-trial interval and a 1-min cut-off period per trial.

All behavioral assays were analyzed by analysis of variance (ANOVA) with age and genotype as fixed factors.

### Enzyme-linked immunosorbent assays

Blood samples were collected, clotted and centrifuged at room temperature to obtain serum samples,

which were aliquoted into microcentrifuge tubes and stored at  $-20^{\circ}\text{C}$ . Serum samples were thawed and diluted in duplicate, and quantitative determination of mouse serum albumin and immunoglobulin (IgG) (Alpha Diagnostic International, San Antonio, TX, USA), IGF-1 (Quantikine, R&D Systems, Inc., Minneapolis, MN, USA) and insulin (Crystal Chem Inc., Downers Grove, IL, USA) were measured using their respective enzyme-linked immunosorbent assay (ELISA) kits according to specific manufacturer instructions. Within 30 min of terminating each reaction assay, optical densities were measured on an ELISA plate reader (SpectraMax Gemini XS, Molecular Devices Corp, Sunnyvale, CA, USA) at a wavelength of 450 nm. Mean absorbance for each duplicate sample was compared with standard curves to obtain concentration values.

#### *Intestinal histology*

Small and large intestine were harvested, rinsed gently in saline to remove food and fecal material, and fixed in 4% buffered formaldehyde for 4 h. After washing twice in phosphate-buffered solution (PBS) for 10 min, tissue samples were then cryoprotected in 30% sucrose in PBS overnight at  $4^{\circ}\text{C}$ . After paraffin embedding, tissues were sectioned at  $10\ \mu\text{m}$  using a sliding microtome, mounted on poly-lysine-coated slides, dried and stained with hematoxylin and eosin (Sigma, St Louis, MO, USA).

#### *Immunocytochemistry*

Small and large intestine were processed for 5-HT<sub>1B</sub>R immunocytochemistry. After cryoprotection with sucrose, intestinal samples were frozen in optimum cutting temperature-embedding medium (Miles Laboratories, Elkhart, IN, USA), cut in  $8\ \mu\text{m}$  sections on a cryostat and thaw mounted on poly-lysine-coated slides. Tissue sections were re-hydrated in potassium-phosphate-buffered solution (KPBS) at room temperature, blocked with 10% normal goat serum and incubated overnight at  $4^{\circ}\text{C}$  with a rabbit polyclonal IgG antibody to the rat 5-HT<sub>1B</sub>R (Acris Antibodies, Hiddenhausen, Germany), diluted 1:100 in KPBS, 0.05% goat serum and 0.1% Triton X-100. This primary antibody recognizes rat, mouse and human epitopes corresponding to amino acids 8–26 and 263–278 of the rat 5-HT<sub>1B</sub>R. The following day, slides were rinsed with KPBS three times and then incubated with a Cy3-conjugated goat anti-rabbit IgG secondary antibody (Jackson ImmunoResearch, West Grove, PA, USA) at room temperature for 2 h at a dilution of 1:800 in KPBS, 0.05% goat serum and 0.1% Triton X-100. Slides were washed three times with KPBS, coverslipped and imaged using an Olympus Fluoview 500 scanning confocal microscope in the Center for Biological Imaging at the University of Pittsburgh. Optimal antibody concentrations were determined by serial dilutions. Controls for the specificity of the antisera consisted of incubation of the tissue with normal rabbit serum substituted for the primary antiserum. Using this substitution, no nonspecific

staining was seen. Positive control consisted of substituting mouse cortex (CTX) for intestinal tissue.

For the dopamine transporter (DAT), a similar protocol was applied on  $20\text{-}\mu\text{m}$  post-fixed coronal brain sections incubated with a rat monoclonal anti-DAT antibody (Chemicon International Inc., Temecula, CA, USA) in the presence of avidin and biotin blocking solutions (Vector Laboratories, Burlingame, CA, USA). Slides were developed with the ABC kit (Vector Laboratories, Burlingame, CA, USA). Optimal development time was determined on parallel sections. All experimental samples were processed simultaneously with pairs of aged-matched WT and KO sections on the same slides. Optical densities were quantified with the ImageJ software (<http://rsb.info.nih.gov/ij/>).

#### *Microarray samples and processing*

Mice were killed by cervical dislocation. Brains were split along the sagittal line, frozen in isopentane and stored at  $-80^{\circ}\text{C}$ . To collect samples, frozen brains were cut on a cryostat to the appropriate anatomical level where series of 1 or 2 mm diameter micro-punches (Sample corer, Fine Science Tools, Foster City, CA, USA) were collected from frontal CTX and striatum (STR) and immediately stored in Trizol reagent (Invitrogen, Carlsbad, CA, USA). CTX samples were collected from prefrontal and cingulate cortices corresponding mostly to non-motor areas between figures 18 and 23 (Bregma  $\sim +2$  to  $+1$  mm) in the Paxinos–Franklin Mouse Brain Atlas.<sup>34</sup> Dorsal STR samples were collected starting at figure 23 in the same atlas (Bregma  $\sim +1$  to  $0$  mm). Total RNA was extracted using the Trizol protocol, cleaned with Rneasy microcolumns (QIAGEN, Hilden, Germany), quantified and verified by chromatography using the Agilent Bioanalyzer system (Santa Clara, CA, USA). Microarray samples ( $n=3\text{--}4$  per age-, genotype- and brain regions; total,  $n\sim 60$  arrays) were prepared according to the manufacturer's protocol. In brief,  $2\ \mu\text{g}$  of total RNA were reverse transcribed and converted into double-stranded complementary DNA (cDNA). A biotinylated cRNA was then transcribed *in vitro*, using an RNA polymerase T7 promoter site, which was introduced during the reverse transcription of RNA into cDNA. Twenty micrograms of fragmented-labeled cRNA sample was hybridized onto MOE 430–2.0 Affymetrix oligonucleotide microarrays (Affymetrix, Santa Clara, CA, USA). A high-resolution image of the hybridization pattern on the probe array was obtained by laser scanning, and fluorescence intensity data were automatically stored in a raw file. To reduce the influence of technical variability, samples were randomly distributed at all experimental steps to avoid any simultaneous processing of related samples. For data extraction, single arrays were analyzed with the Affymetrix Microarray GCOS software. Microarray quality control parameters were as follows: noise (RawQ)  $< 5$  (CTX:  $1.53\pm 0.03$ ; STR:  $1.65\pm 0.05$ ), background signal  $< 100$  (250 targeted intensity for array scaling; CTX:  $46.2\pm 0.9$ ; STR:

45.3±0.8), consistent number of genes detected as present across arrays (CTX: 49.7±0.4; STR: 52.6±0.4), consistent scaling factors (CTX: 1.80±0.05; STR: 1.52±0.06), Actin and GAPDH 3'/5' signal ratios <3 (CTX: ACT, 2.15±0.19, GAPDH, 1.18±0.09; STR: ACT, 1.43±0.04, GAPDH, 0.90±0.03) and consistent detection of BioB and BioC hybridization spiked controls.

#### Array statistical analysis

For statistical analysis, probeset signal intensities were extracted with the robust multi-array average algorithm<sup>35</sup> (<http://www.bioconductor.org>). The 45 101 probesets were reduced to ~20 000 probesets after preprocessing and filtering (present calls ≥10%, coefficient of variation superior than 0.1 and averaged expression ≥20). The 3-month WT and KO groups were bred at a different experimental time and were not combined in a single large-scale analysis.

Denote by  $\{x_{gkti}\}$  the expression intensities from microarray, where  $1 \leq g \leq 45\,101$  labels indexes for genes ( $k=0, 1$ ), for genotype ( $k=0$ : WT;  $k=1$ : KO),  $t=10, 18, 24$  for age and  $i=1, 2, 3, 4$  for biological replicates. Genes with age-related expression changes were selected by the following three analytical procedures.

- *First*, expression intensities of each gene  $g$  were fitted to a two-way ANOVA model in 10-, 18- and 24-month groups and WT and KO groups:  
 $x_{gkti} = \mu_g + \alpha_{gk} + \beta_{gt} + \gamma_{gkt} + \varepsilon_{gkti}$ .
- *Second*, genotype differences were tested (two-group  $t$ -tests) at 3 month of age for all genes identified in (1) and,
- *Third*, one-way ANOVA models within genotype groups (WT and KO) were fitted to genes identified in steps 1 and 2 to characterize the age-related effects in the respective WT or KO experimental groups:  $x_{gkti} = \mu_{gk} + \alpha_{gkt} + \varepsilon_{gkti}$ ,  $k=0,1$ .

The goal of the overall analysis was to use the profiles of expression of large groups of genes as an 'experimental assay' to identify and measure age-related molecular effects, and to assess the cumulative effects of changes over groups of genes (i.e. correlation, functional analysis...). Therefore thresholds for gene selection were kept at medium stringencies ( $P < 0.01$ , changes greater than 20%). This approach has the advantage of allowing the investigation of such patterns, although the extent and levels of correlations may have been slightly underestimated.

#### Mouse-human age-effect correlation

We have previously reported changes in gene expression with age in the human prefrontal CTX using U133Plus-2.0 arrays.<sup>36</sup> Human orthologs of genes with age-effect in the mouse were identified between the MOE-430-2.0 and U133Plus-2.0 arrays using the NetAFFX webtools (Affymetrix, Santa Clara, CA, USA). In the case of multiple human probesets for a

single-mouse probeset, the human probeset with the lowest age-related  $P$ -value was retained. Correlations of age-effects were calculated using  $\log_2$  ratio values. In rodents, the ratios were as described in the text and figures. For humans, the effect of age was calculated as the signal ratio between subjects over 65 years of age versus subjects under 30 years.<sup>36</sup> Similar results were obtained using different threshold criteria for gene selection in the mouse data sets (in Figure 2:  $P < 0.001$ , changes greater than 20%). A similar approach was applied to assess correlations in transcriptome changes in CTX between  $Bdnf^{KO}$  mice<sup>37</sup> and age-related profiles in  $Htr1b^{KO}$  mice, as mouse probesets were directly comparable between the two studies.

#### Age-pattern correlation

To identify patterns of changes in gene expression in relationship to the occurrence of WT/KO behavioral differences (i.e. 10 and 18 months of age), correlation levels were systematically calculated between WT and  $Htr1b^{KO}$  mice gene expression at the 10- and 18-month time points and all possible transcript profiles. Profiles were designed based on two groups (WT and  $Htr1b^{KO}$ ), two time points (10- and 18 months) and three ordinal expression levels (high, medium and low) for a total of  $(3^2)^2 = 81$  possible patterns. The analysis was limited to the 1097 genes with identified age-effects in either experimental groups. With the exception of a very few probesets (See Supplementary Table S5), all identified genes were expressed at the same level at the 3-month time point. Ninety-nine percent of the genes had correlation levels greater or equal to 0.7 with at least one pattern. Patterns were then reduced to three major profiles: (i) initial WT/KO differences at 10 months or 'early' pattern, (ii) initial WT/KO differences at 18 months or 'late' pattern and (iii) overlapping profiles (no WT/KO differences). This approach was more comprehensive than simple group comparisons (i.e. difference or not at 10 or 18 months), although the vast majority of genes displayed correlation levels only with a very few patterns that corresponded closely to the profiles displayed for averaged values in Figure 5.

#### Functional class scoring analysis

See details at <http://www.bioinformatics.ubc.ca/ermine/>.<sup>38,39</sup> Rather than analyzing genes one at a time, gene functional class scoring gives scores to classes or groups of genes, representing the overall effect of age on these groups of genes. Gene groups were organized according to the Gene Ontology (GO) classification<sup>40</sup> and GO groups with greater than 200 or fewer than eight genes were screened out. GO groups were scored as described,<sup>38</sup> using age-related  $P$ -values as gene scores. Briefly, a raw score for each set of genes with a GO family or custom gene group is calculated as the mean of the negative log of the gene scores for all genes in each gene class. When a gene is represented more than once, only the best score is counted. The raw score is transformed into a  $P$ -value for age-effect

on that group by comparing it to an empirically determined distribution of raw scores. This distribution is obtained by randomly generating gene classes of the same size as the class being tested; this is repeated 100 000 times to generate the distribution of scores expected if high gene scores are not concentrated in the class.

#### Real-time quantitative polymerase chain reaction

Real-time quantitative polymerase chain reaction (qPCR) was performed as described previously.<sup>41</sup> In brief, small PCR products (80–120 base-pairs) were amplified in quadruplets on an Opticon real-time PCR machine (MJ Research, Waltham, MA, USA), using universal PCR conditions (65C–59C touch-down, followed by 35 cycles (15 s at 95C, 10 s at 59C and 10 s at 72C)). cDNA (150 pg) was amplified in 20  $\mu$ l reactions (0.3  $\times$  Sybr-green, 3 mM MgCl<sub>2</sub>, 200  $\mu$ M dNTPs, 200  $\mu$ M primers, 0.5 unit Platinum Taq DNA polymerase (Invitrogen, Carlsbad, CA, USA)). Primer dimers were assessed by amplifying primers without cDNA. Primers were retained if they produced no primer dimers or nonspecific signal only after 35 cycles. Results were calculated as relative intensity compared to actin.

#### In situ hybridization

*In situ* hybridization was as described previously.<sup>42,43</sup> Primers were designed using the primer 3 software ([http://frodo.wi.mit.edu/cgi-bin/primer3/primer3\\_www.cgi](http://frodo.wi.mit.edu/cgi-bin/primer3/primer3_www.cgi)) to amplify half of the gene-coding region and half of the 3' untranslated region of the Sirt5 cDNA (NM 178848; base-pairs 510–1144). Primers included SP6 and T7 RNA polymerase promoter tails for sense and antisense *in vitro* transcription from the amplified PCR products. PCR products were amplified from mouse brain cDNA and verified by sequence analysis. Labeled *in vitro* transcription was performed using the Ambion maxiscript kit (Ambion, Inc., Austin, TX, USA) in the presence of <sup>35</sup>S-CTP. Probes were purified using the Qiagen Rneasy kit (Qiagen, Inc., Valencia, CA, USA) and the amount of incorporated radioactivity was quantified on a liquid scintillation counter. *In situ* hybridization was performed on five coronal sections per mouse. Five mice were used per genotype and per age group (3, 6, 18 and 24 months) according to a standard protocol.<sup>42,43</sup> Briefly, slides were incubated for 10 min at room temperature in 4% buffered paraformaldehyde, washed in 0.1 M PBS, serially dehydrated in increasing concentrations of ethanol, and then incubated in hybridization buffer overnight at 56°C in the presence of antisense or sense probe (2 000 000 counts per slide). The following day, the slides were washed, RNase treated, dried and exposed to film. Kodak BioMAX MR film intensities were determined to be optimal after a 4-day exposure. Images were standardized to C<sup>14</sup> standards (ARC-146A and ARC-146D; American Radiolabeled Chemicals, Inc, St Louis, MO, USA) and areas corresponding to CTX and STR were quantified using

the Microcomputer Imaging Device analysis software (Imaging Research, London, ON, Canada).

## Results

### Early onset of age-related motor deficits and reduced longevity in *Htr1b*<sup>KO</sup> mice

*Htr1b*<sup>KO</sup> mice presented no obvious developmental changes,<sup>28,30</sup> exhibited a normal behavior in young adulthood (Figure 1a–d, 2-month time points), but displayed an early onset of characteristic age-related motor decline, which became significant at 6 months of age in the rotarod test and at 12 months in the coat hanger test (Figure 1a and b). Total activity in the open field and the elevated plus maze (EPM) tests were not different from WT controls and declined similarly with age (Figure 1c and d). This early decline in motor behavior in *Htr1b*<sup>KO</sup> mice was not due to learning deficits,<sup>44</sup> as procedural learning curves were essentially parallel between genotypes (Figure 1e). Consistent with previous reports,<sup>28</sup> *Htr1b*<sup>KO</sup> mice displayed normal anxiety-like behavior in young adulthood (Supplementary Figure S1). Assessing the progression of anxiety-related behaviors over time revealed no age-related genotype difference, although the interpretation of these measurements was limited by the very low activity of older animals in both experimental groups in the challenging compartments of the behavioral apparatus (center of open field and open arms of the elevated-plus maze; Supplementary Figure S1).

The first death events occurred between 16 and 20 months of age in *Htr1b*<sup>KO</sup> mice and after 21 months of age in WT mice. *Htr1b*<sup>KO</sup> mice displayed significantly decreased longevity ( $P < 0.0001$ ; Figure 1f), with reductions in maximum (–14%) and average (–19%) life spans. The largest difference was observed at 30 months of age, where ~60% of WT mice but only ~5% of *Htr1b*<sup>KO</sup> mice were still alive. Inspection of complementary log-mortality plots (Figure 1g) and of a Cox proportional hazard model revealed that on average *Htr1b*<sup>KO</sup> mice had a 3.75-fold increase of hazard ratio ( $P < 0.0005$ ). Our analysis also revealed that changes in hazard were time dependent, which means that the increase of hazard could be larger at some points but smaller at other times. However, the averaged slopes of the mortality curves were identical (WT: 0.159 (0.159–0.177), KO: 0.160 (0.160–0.177)) and the time-related differences in estimates were very small, as the *Htr1b*<sup>KO</sup> mortality curve was virtually superimposable on the WT curve (Figure 1g, hatched curve). Thus, together these results demonstrated a shift of longevity and mortality curves toward earlier ages in *Htr1b*<sup>KO</sup> mice, and suggested a causative and modulatory role for 5-HT in age-related motor behavior and longevity.

### The 'age-related' phenotype of *Htr1b*<sup>KO</sup> mice appears mediated by brain mechanisms

The 5-HT<sub>1B</sub>R is the main 5-HT presynaptic auto-receptor in the brain<sup>27</sup> and has limited functions in

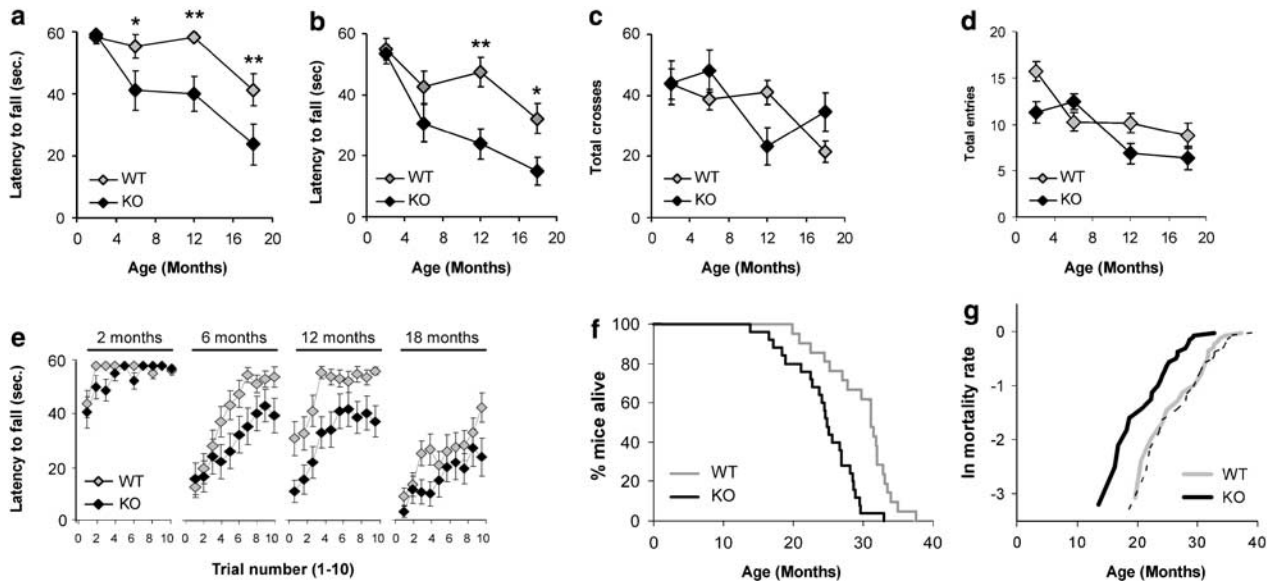


**Figure 1** Early onset of age-related motor decline and reduced longevity in *Htr1b*<sup>KO</sup> mice. **(a and b)** *Htr1b*<sup>KO</sup> mice displayed early age-related motor impairment in the rotarod test (**(a)** latency to fall:  $F_{3,117} = 11.37$ ,  $P < e^{-6}$ ; genotype effect:  $F = 15.04$ ,  $P < 0.0005$ ; genotype\*age:  $F = 2.05$ ,  $P = 0.11$ ) and the coat hanger test (**(b)** latency to fall:  $F_{3,117} = 8.67$ ,  $P < 0.0001$ ; genotype effect:  $F_{1,120} = 16.29$ ,  $P < 0.0001$ ; genotype\*age:  $F_{3,117} = 1.98$ ,  $P = 0.12$ ). *Post hoc* tests: \* $P < 0.05$ , \*\* $P < 0.005$ . **(c and d)** Total activity decreased with age in WT and *Htr1b*<sup>KO</sup> mice in the open field (OF) **(c)** and EPM **(d)** tests (age-effect. OF:  $F = 4.12$ ,  $P = 0.008$ ; EPM:  $F = 20.78$ ,  $P < e^{-5}$ ), although variability in the 12- and 18-month age groups suggested a potential age\*genotype interaction (genotype\*age-effect. OF:  $F = 3.09$ ,  $P = 0.03$ ; EPM:  $F = 3.4$ ,  $P = 0.02$ ; all other effects,  $P > 0.05$ ). Different cohort of mice was used for each time point to avoid memory savings between experiments (**a–d**:  $n = 13–18$  per group and per age). **(e)** Procedural learning curves in the rotarod test were essentially similar, but reached lower maximal values in *Htr1b*<sup>KO</sup> mice (see **(a)**). **(f)** Kaplan–Meyer survival curves revealed a significant decreased in longevity in *Htr1b*<sup>KO</sup> mice ( $P < 0.0001$ ). **(g)** Mortality curves: *Htr1b*<sup>KO</sup> mice displayed a 3.75-fold increased hazard ratio ( $P < 0.0005$ ). Hatched curve represents *Htr1b*<sup>KO</sup> mortality curve superimposed on the WT curve (**f and g**, WT,  $n = 21$ ; KO,  $n = 24$ ).

the periphery. Thus we hypothesized that the age-related phenotype might be mediated by central mechanisms, but first, we investigated selected peripheral systems as potential contributors to the phenotype. WT and *Htr1b*<sup>KO</sup> mice had indistinguishable morphologic features at all ages, including body weights (Figure 2a). Mild alopecia and kyphosis appeared in both genotypes after 2 years of age (not shown). Necropsy procedures revealed no genotype changes in organ's appearance or weight (not shown), including in kidney and lung, two organs with reported roles for 5-HT<sub>1B</sub>R signaling.<sup>45,46</sup> 5-HT modulates gastrointestinal and immune functions, but the 5-HT<sub>1B</sub>R plays little-to-no role in these systems.<sup>47,48</sup> Correspondingly, 5-HT<sub>1B</sub>R immunoreactivity was undetected in the intestinal tract (not shown) and no changes in colonic morphology were identified (Figure 2b). ELISA immunoassays on serum obtained from young and old mice revealed normal albumin content (Figure 2c), suggesting normal absorptive capacity in *Htr1b*<sup>KO</sup> mice as compared to controls.

Due to the endocrine regulation of aging<sup>49</sup> and potential interaction with the 5-HT system,<sup>25</sup> we measured circulating levels of insulin and IGF-1. Both hormones displayed lower levels in young and old KO mice when compared to age-matched control mice (Figure 2c and d), although these differences reached statistical significance only for insulin.

Serum levels for insulin increased with age in *Htr1b*<sup>KO</sup> mice, suggesting that the lower levels in young KO mice were not due to primary deficits in hormone production. The direction of changes also suggests that hormonal levels are not mediating the age-related phenotype of *Htr1b*<sup>KO</sup> mice for two reasons. First, increased levels above normal, rather than lower insulin levels, are associated with deleterious effects of aging.<sup>50</sup> Second, earlier studies in model organisms,<sup>49</sup> including mice,<sup>51</sup> predict a protective effect of decreased IGF-1 levels against aging.

Finally, an immunoassay for circulating IgG revealed a smaller age-related increase in IgG levels in serum of old KO mice (2.3-fold increase) versus age-matched WT controls (9.1-fold increase; Figure 2f), thus suggesting a reduced inflammatory load, or reduced recruitment of the immune system in aging *Htr1b*<sup>KO</sup> mice. Thus, combined with the limited functions of 5-HT<sub>1B</sub>R in the periphery, these results suggested that the age-related behavioral phenotype and reduced longevity of *Htr1b*<sup>KO</sup> mice may have originated from a central deficiency.

#### *Dopaminergic terminal density and area are not affected in old Htr1b<sup>KO</sup> mice*

In the brain, 5-HT<sub>1B</sub>R modulates the synaptic release of 5-HT in serotonergic projection fields, but also acts as a heterologous autoreceptor indirectly regulating

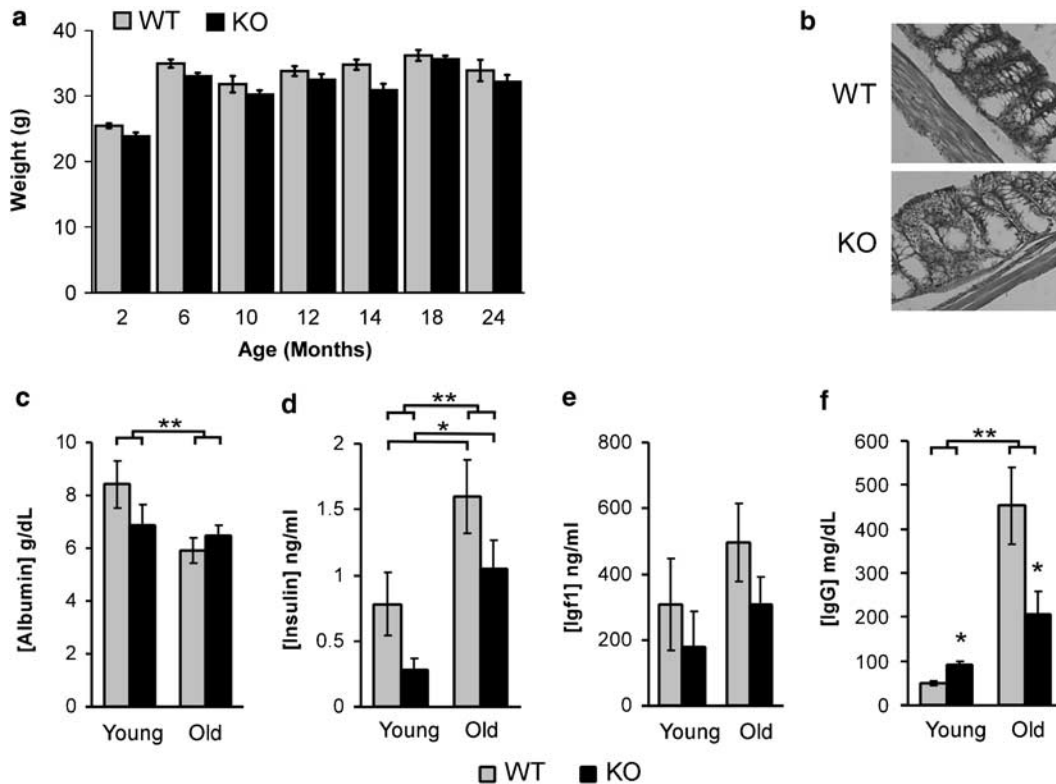


**Figure 2** Peripheral markers in *Htr1b*<sup>KO</sup> and WT mice. (a) Body weight ( $n=14$ – $16$  per group,  $P>0.05$ ). (b) Colon mucosal and smooth muscle layers and lumen were equivalent in WT and KO mice (hematoxylin/eosin staining; representative sections from old WT and KO groups). (c–e) Serum levels of albumin (c), insulin (d), insulin-like growth factor 1 (IGF-1; e) and IgG (f). (c–e): Young (3 months; WT,  $n=5$ ; KO,  $n=5$ ) and old (18 months; WT,  $n=6$ ; KO,  $n=6$ ). Statistical significance: main-age effects for albumin ( $F_{1,22}=10.2$ ,  $P=0.005$ ), insulin ( $F_{1,22}=11.8$ ,  $P<0.005$ ) and IGF-1 ( $F_{1,22}=21.27$ ,  $P<0.001$ ). Main genotype effect for albumin ( $F_{1,22}=4.4$ ,  $P=0.08$ ), genotype\*age interaction ( $F_{1,22}=9.2$ ,  $P=0.02$ ). Main genotype effect for insulin ( $F_{1,22}=5.02$ ,  $P<0.05$ ) and age–genotype interaction for IgG ( $F_{3,22}=6.5$ ,  $P<0.05$ ). All other effects,  $P>0.05$ . *Post hoc* tests; \*\* $P<0.01$ , \* $P<0.05$ . Error bars represent s.e.m.

dopamine (DA) functions. Indeed, *Htr1b*<sup>KO</sup> mice displayed elevated basal DA levels and increased striatal overflow after cocaine challenge,<sup>31</sup> suggesting potential interactions between DA and the age-related motor phenotype. Using immunohistochemistry against the DA transporter, we found no differences in DA terminals density in the ventral or dorsal STR of young and old WT or KO mice ( $P>0.5$ ) (Figure 3a and b). DA terminal striatal areas were also unchanged between genotype groups (Figure 3c). Representative figures and measurements are provided at the 18-month time point, long after the onset of behavioral differences (6–10 months of age) and corresponding to the time of early onset of death events in the KO group. Thus, together these results suggested that the early adulthood onset of the motor phenotype in *Htr1b*<sup>KO</sup> mice was not due to a structural downregulation of the DA system.

#### *Altered gene expression in the brain of aging Htr1b<sup>KO</sup> mice corresponds to 'normal' aging*

Altered 5-HT signaling in *Htr1b*<sup>KO</sup> mice could induce brain deficits that are detrimental to long-term brain homeostasis and survival and that are yet unrelated to

age-related processes. Thus, as aging is accompanied by characteristic changes in gene expression in the brain,<sup>36,52,53</sup> we predicted that the 'molecular signature of aging' might occur earlier in *Htr1b*<sup>KO</sup> mice. To this goal we first investigated the nature of life-long gene expression changes in CTX and STR, two brain areas with well-characterized roles for the 5-HT<sub>1B</sub>R, and then assessed putative differences in the trajectories of age-related changes in *Htr1b*<sup>KO</sup> mice.

Roughly twice as many genes were affected in correlation with age in CTX of *Htr1b*<sup>KO</sup> mice, compared with WT mice, with fewer genes affected in STR in both experimental groups (Figure 4a; Supplementary Tables S1 and S2). Despite a considerable overlap (especially in CTX), some genes were identified only in the WT or in the KO group, reflecting either the presence of different age-related effects, or the limitation of the analytical procedures at detecting milder effects in one or the other group. To address this question, we hypothesized that if selected genes were age related, then the overall changes in transcript levels should correlate across groups, regardless of whether genes passed statistical thresholds or not. Indeed, genes identified only in

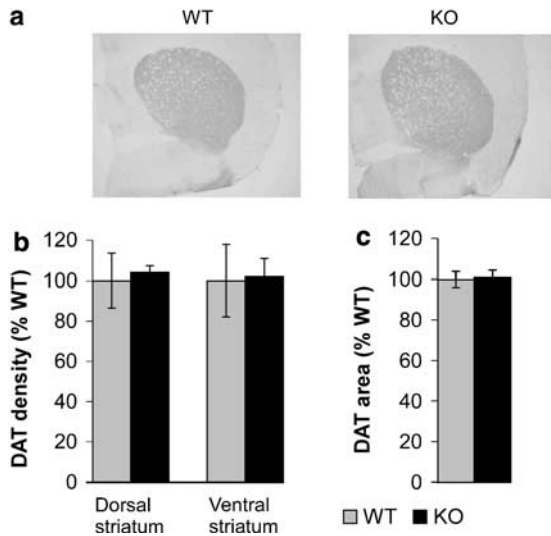


**Figure 3** Intact dopaminergic terminal density in old *Htr1b*<sup>KO</sup> mice. (a) Representative photographs of DAT immunohistochemistry in 18-month-old WT and *Htr1b*<sup>KO</sup> mice ( $n=4$  per group,  $P>0.05$ ). (b) DAT immunoreactivity density. (c) DAT striatal area (similar results were obtained at 3, 6 and 24 months of age).

*Htr1b*<sup>KO</sup> mice demonstrated high correlation levels with the effect of aging on the same genes in WT mice (Figure 4b, middle panel), and conversely age-related changes in transcript levels identified only in WT mice correlated highly with changes in KO mice (Figure 4b, left panel), thus revealing that a similar pool of genes was affected across genotypes. The higher slope values in the correlation graphs of KO-only selected genes (CTX, KO=1.5, WT=1.2; STR (not shown), KO=2.3, WT=1.4) further suggested a larger and more extensive age-effect in *Htr1b*<sup>KO</sup> mice. Interestingly, correlations were the highest when comparing 18-month-old KO mice to 24-month-old WT mice (Figure 4c), suggesting that *Htr1b*<sup>KO</sup> mice reached a pronounced age-effect earlier than WT mice. This ‘maximum’ age-effect corresponded to the period where death events started to occur in *Htr1b*<sup>KO</sup> mice (Figure 1f).

#### Mouse–human phylogenetic conservation of age-effect in brain CTX

Comparing results to our previous study of the molecular correlates of aging in the human brain,<sup>36</sup> we identified highly significant correlations between age-related effects in WT or *Htr1b*<sup>KO</sup> mice and the two investigated areas of the human prefrontal CTX (Figure 4d–f). Mouse–human correlations of age-effects increased from 18 to 24 months in WT mice, but again were highest for 18-month-old *Htr1b*<sup>KO</sup> mice (Figure 4e). Selected genes with conserved age-effects are displayed in Figure 4f and in the Supplementary Information (Supplementary Table S3). Together, these results demonstrated a phylogenetic conservation of age-effect in mammalian CTX and confirmed

the age-related nature and early peak of the brain molecular phenotype of *Htr1b*<sup>KO</sup> mice.

#### Early occurrence of the age-related gene expression signature in *Htr1b*<sup>KO</sup> mice

With very few exceptions (see last paragraph), all identified genes were expressed at similar levels in WT and KO mice at 3 months of age (Figure 5, 3-month time point), indicating that the molecular correlates of the differential age-related phenotype in *Htr1b*<sup>KO</sup> mice were initiated later in adulthood, and consistently with the lack of behavioral differences in young adulthood. As predicted, investigating the appearance and progression of age-related changes revealed that over 98% of individual genes affected in CTX displayed early changes in *Htr1b*<sup>KO</sup> mice when compared to WT controls. Changes (25.6%) occurred initially at 10 months (Figure 5a and b, ‘early’ pattern) and 72.6% at 18 months of age (Figure 5c and d, ‘late’ pattern). Likewise, over 97% of age-related genes identified in STR displayed similar anticipated age-related profiles in *Htr1b*<sup>KO</sup> mice (not shown). This early onset of age-related pattern is illustrated for glial fibrillary acidic protein (Gfap; Figure 5e and f), a marker of age- and brain-related events<sup>54</sup> (i.e. inflammation), which displayed a ‘late’ pattern of changes, with initial WT–KO differences at 18 months of age.

The presence of different age-related patterns of changes in transcript levels raised the question as to whether specific biological functions were associated with these patterns, and could thus have mediated the early onset of behavioral changes in *Htr1b*<sup>KO</sup> mice. To address this question, we (a) systematically identified groups of related genes displaying high representation of age-affected genes,<sup>36,39</sup> (b) compared results between WT and KO mice and (c) further investigated whether any of the identified gene groups displayed over- or under-representation of genes with changes occurring in parallel to the onset of behavioral differences (i.e. ‘early’ or ‘late’ patterns). The cumulative effect of aging on gene groups was assessed according to the GO classification<sup>40</sup> and is presented in a color-coded fashion for the 25 most affected gene groups in WT or *Htr1b*<sup>KO</sup> mice (Figure 5g and Supplementary Table S4). The nature of the identified gene groups revealed that very similar biological functions were affected during aging in WT and *Htr1b*<sup>KO</sup> mice, albeit with minor differences. Translation-related gene groups (blue bars in Figure 5g) were prominent in both groups, but displayed increased ‘ranked’ representation in *Htr1b*<sup>KO</sup> mice, whereas the representation of inflammation-related gene groups (red bars in Figure 5g) was decreased in *Htr1b*<sup>KO</sup> mice, in reminiscence of previous evidence suggesting reduced inflammation in the periphery (Figure 1e). Results are presented for CTX and were highly similar in STR (not shown). Importantly, the proportion of genes with ‘early’ or ‘late’ onset of WT/KO changes differed only marginally from their expected proportions within

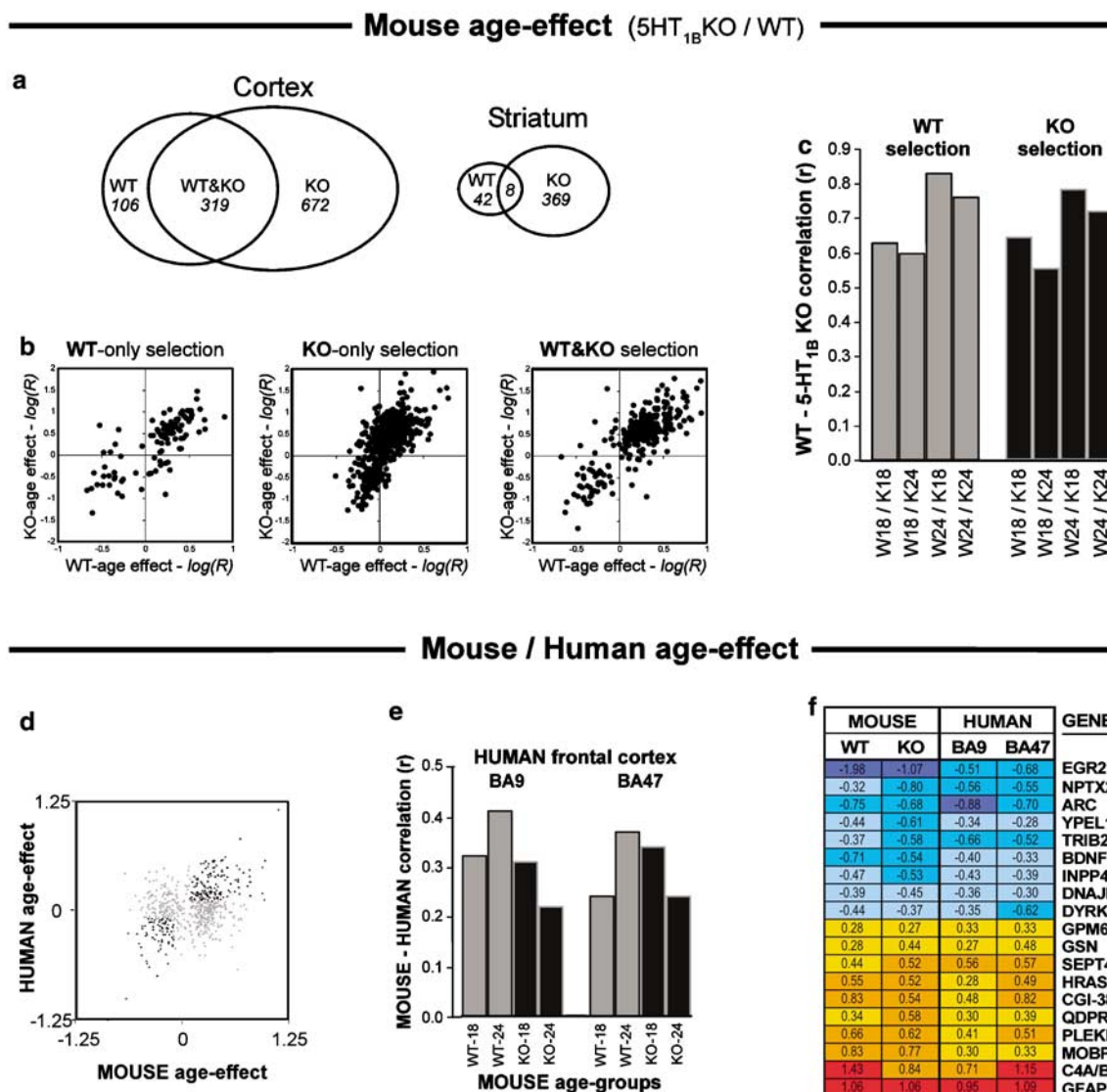


**Figure 4** Correlation of age-related gene expression ‘signatures’ in the brains of WT and *Htr1b*<sup>KO</sup> mice, and phylogenetic conservation of age-effect between mice and humans. (**a–c**) WT/*Htr1b*<sup>KO</sup> age-effect comparison. (**a**) Venn diagrams of age-related transcript changes in CTX and STR ( $n = 3–4$  arrays per age-, genotype- and brain regions; total,  $n = \sim 60$  arrays). (**b**) Correlation graphs between age-effects ( $\text{LogR} = \log_2 \text{Old/Young}$ ) in CTX between genes identified only in WT ( $n = 106$ , left), only in KO ( $n = 672$ , middle) and in both groups ( $n = 319$ , right). (**c**) Correlation levels ( $r$ ) of age-effects between indicated WT and *Htr1b*<sup>KO</sup> age groups. All  $P < 0.0001$  (**d–f**) Mouse/human age-effect comparison. (**d**) Age-effect correlation graph between genes identified in the mouse and for which age-related expression levels of orthologous genes were available in the human CTX.<sup>36</sup> Black dots indicate genes with most conserved age-effects that are likely to support a large proportion of the overall correlation (see (**f**) and Supplementary Table S3). (**e**) Correlation levels between age-related transcript changes in WT or *Htr1b*<sup>KO</sup> mouse CTX and two areas of the human prefrontal CTX. All  $P < 0.005$ , except WT18 versus BA47,  $P = 0.01$ . Correlations were based on age-effect in rodent ( $P < 0.001$ ) and identifiable human orthologs (WT,  $n = 88$  genes; KO,  $n = 271$  genes). (**f**) Selected genes with conserved age-effects in CTX between mouse and human. Values are in average  $\log_2$  (old/young ratio) (red: increased; blue: decreased). See Supplementary Table S3 for additional genes and details. BA9/47, Brodmann areas 9/47.

the five main identified age-related functions (Figure 5h), with the exception of translation-related gene groups that displayed significantly more genes with late-onset differences. Genes with early WT/KO age-related differences were slightly, but non-significantly, over-represented in inflammation-related functions.

Taken together, results from our temporal and functional analyses of age-related changes in gene expression did not identify any specific biological function as the potential source or mediator of the early onset of the age-related phenotype, but rather suggested a global and early shift of the molecular signature of aging in the brain of *Htr1b*<sup>KO</sup> mice.

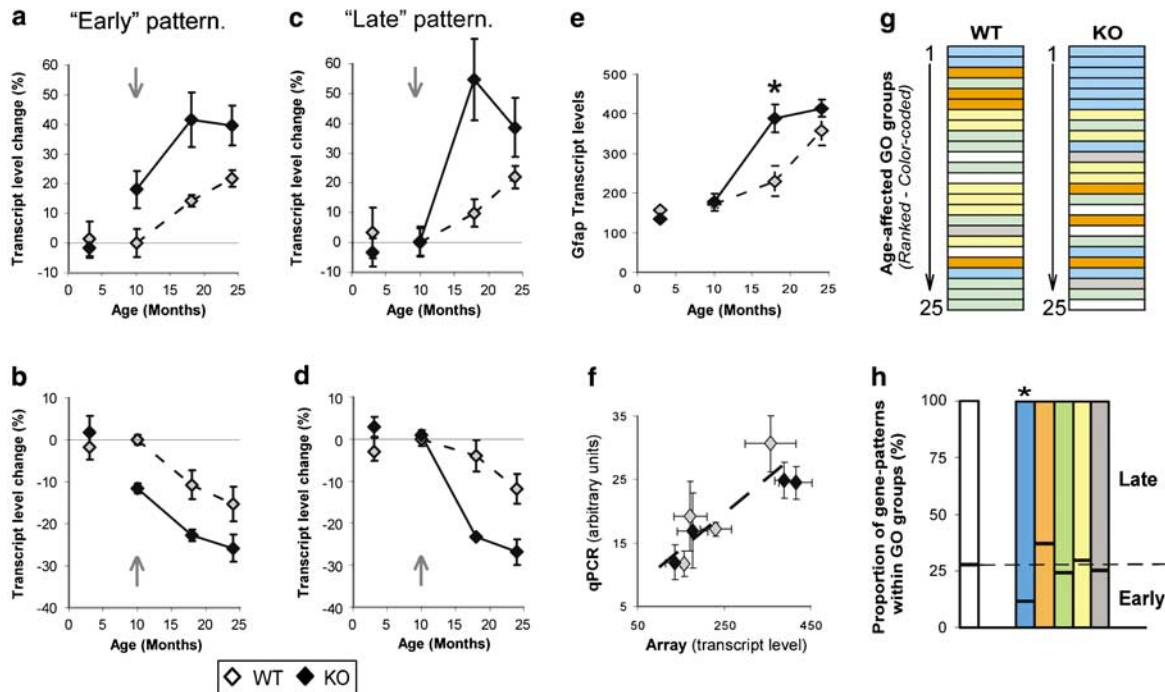


**Figure 5** Over 98% of age-related genes displayed early onset of age-related trajectories in *Htr1b*<sup>KO</sup> mice. (a–d) Averaged transcripts profiles for genes with onset of age-related effects in KO mice occurring initially at 10 months ('Early': 198 increased (a) and 81 decreased (b) genes; 25.6% of age-related genes) or 18 months ('late': 670 increased (c) and 126 decreased (d) genes; 72.6% of age-related genes), compared to the onset of behavioral differences (vertical gray arrow). Less than 2% of age-affected genes had similar profiles in WT and KO mice (not shown). Values are in percentage of WT levels. The 3-month-old groups used for array analysis were bred at a different time and analyzed separately. (e) *Gfap* age-related transcript profiles as an example of 'late' pattern (age-effect,  $P < 0.0005$  in WT and KO; \*WT/KO at 18 month,  $P < 0.05$ ). (f) Confirmation of altered *Gfap* transcript levels by real-time qPCR: Array/qPCR correlation ( $r = 0.87$ ,  $P = 0.005$ ). Values are mean  $\pm$  s.e.m. (g and h) Functional analysis of molecular aging. (g) The 25 most affected color-coded gene groups in WT and *Htr1b*<sup>KO</sup> mice are regrouped in five main functions: translation (blue), inflammation (red), metabolism (green), cell growth (yellow), cellular respiration (gray), miscellaneous (white). Details in Supplementary Table S4. (h) Proportional representation of genes with 'early' (10 months) or 'late' (18 months) patterns of initial WT–KO differences in age-related trajectories within the main age-related functions. \* $P < 0.001$ , difference from expected proportions (white column and hatched bar).

### A role for *Bdnf* in age-related transcriptome changes and in the *Htr1b*<sup>KO</sup> molecular phenotype?

Altered neurotrophic function, including 5-HT/*Bdnf* interactions, has been suggested to mediate some of the age-related changes occurring in the brain.<sup>25</sup> Here, we confirmed the previously reported down-regulation of *Bdnf* transcripts with age in CTX<sup>36,43,55</sup> (WT:  $-1.63$ -fold change,  $P = 0.006$ ; KO:  $-2.24$ -fold change,  $P = 0.002$ ; Supplementary Tables S1 and S3) and showed that changes followed an 'early' pattern in *Htr1b*<sup>KO</sup> mice (Supplementary Table S1), thus suggesting a potential causative role for altered *Bdnf* function in the *Htr1b*<sup>KO</sup> age-related phenotype. Therefore, to investigate the potential contribution of *Bdnf* to the molecular phenotype of *Htr1b*<sup>KO</sup> mice, we took advantage of a recent report describing CTX gene expression changes occurring downstream from altered *Bdnf* function in *Bdnf* KO mice (embryonic or adult *Bdnf*<sup>KO</sup>, see<sup>37</sup>) and investigated similarities between *Bdnf*- and age-induced transcriptome changes. In particular, if changes in *Bdnf* function participated in the age-related *Htr1b*<sup>KO</sup> molecular

phenotype, then the effect of *Bdnf*<sup>KO</sup> on altered gene transcripts would correlate with the effect of aging, and should mostly follow an early pattern of changes in *Htr1b*<sup>KO</sup> mice. Here, we identified a moderate, but significant, correlation between changes in *Bdnf*<sup>KO</sup> mice and age-related changes in *Htr1b*<sup>KO</sup> or WT mice ( $r = \sim 0.20$ ,  $P < 0.05$ ). Correlations with age-related profiles were slightly higher for adult ( $r = 0.22$ ,  $P < 0.05$ ,  $n = 98$  genes) versus embryonic *Bdnf*<sup>KO</sup>-induced changes ( $r = 0.17$ ,  $P < 0.05$ ,  $n = 173$  genes). Correlations with *Bdnf*<sup>KO</sup>-induced changes were also slightly higher when compared to age-related changes in *Htr1b*<sup>KO</sup> ( $r = 0.23$ ,  $P < 0.05$ ,  $n = 271$  genes) versus WT mice ( $r = 0.20$ ,  $P < 0.05$ ,  $n = 271$  genes). Importantly, genes affected by both *Bdnf* and aging displayed age-related trajectories that were evenly distributed between 'early' and 'late' patterns on WT/*Htr1b*<sup>KO</sup> differences (i.e. 50% 'early' patterns genes), suggesting that *Bdnf* downregulation did not play a major role in the early onset of age-related events in *Htr1b*<sup>KO</sup> mice.

Together, these comparative studies revealed a potential active role for Bdnf in age-related changes, as altered gene expression induced by decreased Bdnf correlated with aspects of the molecular correlates of aging in the brain ( $r = \sim 0.20$ ,  $P < 0.05$ ). However, our studies also suggested that the early age-related phenotype in *Htr1b*<sup>KO</sup> mice was independent of the role of Bdnf in aging.

#### Increased age-related sirtuin 5 gene expression

What possible mechanism could induce the early onset of age-related events in *Htr1b*<sup>KO</sup> mice? Out of  $\sim 45\,000$  transcripts tested, only eight gene transcripts displayed consistent genotype differences in CTX and STR (Supplementary Table S5), including at the 3-month time point that preceded the behavioral differences. Two of these probes corresponded to the sirtuin 5 gene (*Sirt5*), which belongs to a family of protein deacetylases that regulate life span in yeast, *Caenorhabditis elegans* and *Drosophila*.<sup>56</sup> Increased *Sirt5* transcripts were confirmed by qPCR and *in situ* hybridization and displayed a pattern of increased levels in *Htr1b*<sup>KO</sup> mice, converging toward WT levels at 24 months (Figure 6). The role of sirtuin genes in replicative and chronological aging in lower eukaryotes and mammalian cells is complex<sup>57,58</sup> and whether the reported increased *Sirt5* transcripts, and potentially sirtuin 5 function, may mediate the early onset of aging in *Htr1b*<sup>KO</sup> mice or represent an early adaptive mechanism is currently under investigation.

### Discussion

Together our studies have demonstrated that altering 5-HT signaling through the disruption of the 5-HT<sub>1B</sub> presynaptic autoreceptor can modulate the onset of selected age-related events in the central nervous system. We have shown that the lack of 5HT<sub>1B</sub>R-mediated signaling induced both an early age-related motor decline (Figure 1) and an early shift of the characteristic gene expression signature of aging in the brain (Figure 5), ultimately resulting in decreased longevity (Figure 1). Our results also suggested that the age-related phenotype in *Htr1b*<sup>KO</sup> mice may have originated in the brain, as peripheral markers revealed no effect (intestinal tract), or changes suggesting protection or adaptive mechanisms (insulin and IGF-1 systems, Figure 2) against deleterious aspects of the early onset of age-related events. As aging can be viewed as the accumulation of a variety of events that together create in essence a chronic challenge to the brain, and since the 5-HT system is a key system for homeostatic control and adaptation to stress,<sup>59</sup> we have provided here evidence supporting the notion that the interaction of 5-HT with this challenge influences age-dependent behavior and molecular events.

Investigating the nature and progression of age-related changes in brain gene expression throughout the adult life, we have uncovered profound changes in *Htr1b*<sup>KO</sup> mice, which were characteristic of an early

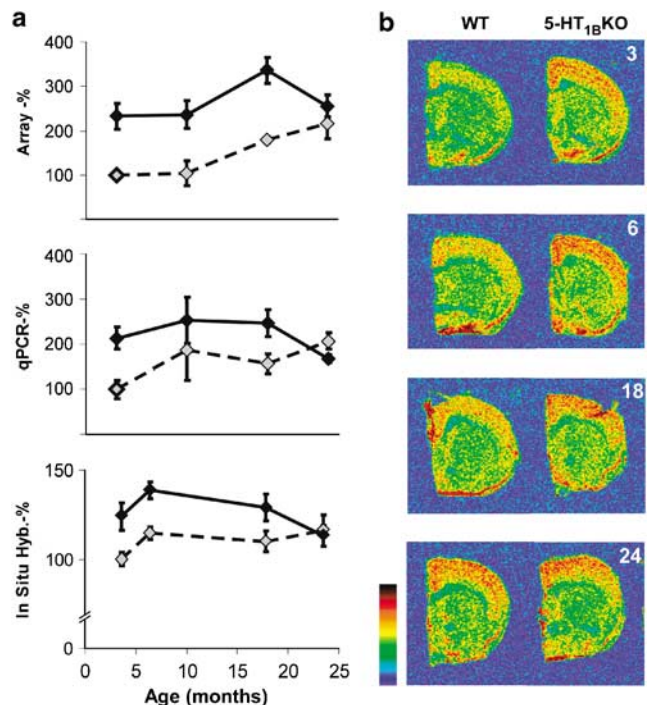


**Figure 6** Upregulated *Sirt5* gene expression in CTX of *Htr1b*<sup>KO</sup> mice. (a) Microarray (top), qPCR (middle) and *in situ* hybridization (ISH, bottom) analyses revealed significant increased *Sirt5* transcript levels in *Htr1b*<sup>KO</sup> mice, with normalized differences at 24 months of age. Smaller differences by ISH were mostly due to *Sirt5* expression throughout the brain, which precluded background subtraction and likely underestimated specific signal differences. All values are in percentage of young WT controls. Genotype effect: array,  $P < 0.01$ ; qPCR,  $P < 0.05$ ; ISH,  $P < 0.01$ . Pair-wise correlations (array–qPCR–ISH), all  $r > 0.65$ ,  $P < 0.05$ . (b) Representative color-coded photomicrographs of *Sirt5* <sup>35</sup>S-ISH at 3, 6, 18 and 24 months of age. Color barcode indicates increased signal intensity.

onset of brain molecular aging (Figure 4). The age-related nature and early onset of the brain molecular phenotype in *Htr1b*<sup>KO</sup> mice was further confirmed by cross-species comparisons with the correlates of aging in the human brain.<sup>36</sup> Indeed age-related changes occurring in the CTX of WT or *Htr1b*<sup>KO</sup> mice significantly predicted age-related changes in two areas of the human CTX, and identified numerous individual genes with similar age-effects across species (Figure 4 and Supplementary Table S3), thus demonstrating a phylogenetic conservation of the molecular correlates of aging from mouse to human. These analyses confirmed numerous prior findings at the level of individual genes (e.g. *Gfap*, *Bdnf*, *MOBP*, complement activation, etc.; Supplementary Table S3), but to our knowledge, this is the first large-scale demonstration of a rodent–human phylogenetic conservation of age-effect in the mammalian CTX, thus validating the use of rodent models to recapitulate aspects of aging of the human brain. Importantly, these cross-species comparisons confirmed the age-related nature and the early onset of the brain

molecular phenotype in *Htr1b*<sup>KO</sup> mice, as *Htr1b*<sup>KO</sup>–human correlations of age-effect reached similar levels than in WT–human comparisons, albeit at an earlier age (Figure 4e).

Imaging and molecular studies suggest that age-related changes are continuous and progressive throughout the human adult life span.<sup>1,2,36,53</sup> Here we provided evidence supporting the notion of a ‘maximum’ age-related molecular effect. Indeed, *Htr1b*<sup>KO</sup> mice reached an apparent peak in age-related changes in gene transcript levels at 18 month of age (Figure 5), which had not yet been attained at the latest time point investigated in WT mice (24 month of age). Interestingly, the timing of this ‘maximum’ age-effect corresponded to the age where death events started to occur in the KO group, suggesting a failure of the system at maintaining proper homeostasis past this point. Indeed, the decreased correlations of age-related transcriptome profiles that were observed between very old *Htr1b*<sup>KO</sup> mice and either control mice or human subjects (Figure 2) may have reflected the presence of secondary and less-specific events occurring beyond a certain maximum age-related effect. Nevertheless, despite the potential occurrence of a late breakdown in homeostasis, our results demonstrated mostly a parallel and early age-related phenotype in *Htr1b*<sup>KO</sup> mice. This trajectory was different from the exponential acceleration in age-related phenotypes and mortality that is commonly observed in mouse models of peripheral/somatic age-related mechanisms.<sup>60–63</sup> In particular, the increased hazard ratio in *Htr1b*<sup>KO</sup> mice (Figure 1h) appears to be mostly due to a shift of death events toward earlier ages, rather than a progressive increase in frailty leading to an exponential homeostatic failure.<sup>60–63</sup> This parallel, rather than exponential, trajectory is consistent with a progressive and cumulative effect over time, rather than an acute and early mechanistic switch leading to a catastrophic failure of the system. Here we suggest that this parallel age-related trajectory in *Htr1b*<sup>KO</sup> mice is consistent with an altered capacity of the 5-HT system to initially respond to the chronic challenge that is formed over time by various events occurring during brain aging. Indeed, as typical longevity and molecular curves display early ‘buffer’ periods where the cumulative effects of aging are not yet observed (i.e. 3- to 12-month behavioral and gene expression time points in WT), *Htr1b*<sup>KO</sup> mice display a reduced ‘buffer’ period (3-months time point), resulting in an early onset, rather than altered progression, of age-related phenotypes.

To identify potential mechanisms mediating the early onset of the *Htr1b*<sup>KO</sup> age-related phenotype, we proceeded with both unbiased surveys of cellular and biological functions and with directed evaluation of markers for candidate biological systems. Systematic analyses of functional relationships and of temporal patterns between age-affected genes (Figure 5) did not identify any novel biological functions being recruited during aging in *Htr1b*<sup>KO</sup> mice, but rather suggested a global and early onset of the molecular

signature of ‘normal’ aging in the brain of *Htr1b*<sup>KO</sup> mice. Regarding candidate systems, a leading hypothesis for age-related mechanisms centers on the role of oxidative stress and inflammation, as mediators of neuronal damage and subsequent increase in reactive astrocytes.<sup>14,64</sup> Here, our combined observations of decreased ranked representation of inflammation-related functions in the brain, of late appearance of WT/KO differences of a cellular marker of inflammation (*Gfap*; Figure 5e and f) and of evidence of reduced peripheral inflammation (*IgG*, Figure 2f) did not support the notion that inflammation-related events mediated the early onset of aging in *Htr1b*<sup>KO</sup> mice. Nevertheless, we cannot rule out the possibility that additional peripheral mechanisms may have contributed to the phenotype, especially in the absence of more direct measurements of reactive oxygen species-mediated damage such as lipid peroxidation and protein carbonylation, which may have contributed to the shortened life expectancy.

*Bdnf* is a neurotrophic factor supporting neuronal functions during development and in the mature brain. Correlative evidence of decreased *Bdnf* transcript levels with age in the human frontal CTX<sup>36,43,55</sup> has suggested the possibility of a causative role in brain aging. Here, we confirmed the downregulation of *Bdnf* with aging in the mouse CTX. We also identified a modest but significant correlation between the effects of *Bdnf* hypofunction in *Bdnf*<sup>KO</sup> mice<sup>37</sup> and the gene expression correlates of aging in mouse CTX ( $r = \sim 0.20$ ,  $P < 0.05$ ), suggesting that aspects of aging in the brain may occur as a consequence of downregulated *Bdnf* function. However, although interactions between 5-HT and *Bdnf* have been documented<sup>65</sup> and hypothesized to both concur with IGF-1 to influence age-related events,<sup>25</sup> our results suggest an age-related phenotype in *Htr1b*<sup>KO</sup> mice that is independent of *Bdnf* function.

On the other hand, our studies provided supporting evidence for potential interacting mechanisms between 5-HT and the previously identified age-related IGF-1 and sirtuin systems. A nonsignificant trend toward downregulated levels of circulating IGF-1 levels in *Htr1b*<sup>KO</sup> supports the notion of 5-HT/IGF-1 interaction during aging. In this case, lower IGF-1 levels would be protective against aging<sup>51</sup> and thus it is not known whether lower IGF-1 levels represented a direct consequence of altered 5-HT function or rather a reactive/protective process against the detection of an early onset of age-related symptoms, as recently hypothesized for age-related processes in peripheral organs.<sup>66</sup> Interestingly, a clear upregulation of sirtuin 5 gene expression was identified in the brain of *Htr1b*<sup>KO</sup> mice. Sirtuin genes are major cellular components of age-related pathways; however, their role in replicative and chronological aging in lower eukaryotes and mammalian cells is complex.<sup>57,58</sup> The role of altered *Sirt5* transcripts in the age-related phenotype in *Htr1b*<sup>KO</sup> mice is currently under investigation, including as a potential mediator of 5-HT control over homeostasis, or as an early

mechanism for altering the onset of age-related phenotypes, since Sirt5 transcript changes preceded the appearance of age-related behavioral and molecular changes. Nevertheless, it suggests that the differentiated central nervous system may share common molecular and/or cellular components with age-related mechanisms in peripheral somatic tissues.

Although the observed phenotype originated from a deficiency in 5-HT-mediated presynaptic inhibition, a limitation in the analysis of potential mechanisms supporting the observed phenotype resides in the fact that the deletion of this receptor altered the kinetics of the 5-HT system,<sup>27,31,32</sup> and thus could have influenced the behavior, molecular and longevity phenotypes through altered signaling at other 5-HT receptors. Therefore, the observed phenotypes should be considered in the context of altered 5-HT-mediated functions in *Htr1b*<sup>KO</sup> mice. This observation relates to our initial choice of the *Htr1b*<sup>KO</sup> mice for investigating the role of 5-HT into aging, as we hypothesized that a disrupted 5-HT homeostasis may initially more closely model the evidence of a deregulated control of 5-HT during aging (see Introduction). Moreover, other neurotransmitters systems interacting with 5HT<sub>1B</sub>R and not investigated here may have played a role in the mutant phenotype. In particular, changes in cholinergic functions may have occurred, as suggested by Buhot *et al.*,<sup>44</sup> in view of complex changes in memory functions in aging *Htr1b*<sup>KO</sup> mice.<sup>44</sup>

The presence of an early deficit in motor behavior was consistent with the role of 5-HT<sub>1B</sub>R in motor function.<sup>28</sup> The distribution and functional contribution of 5-HT<sub>1B</sub>R in the spinal cord and cerebellum are low,<sup>67,68</sup> whereas the nature of the phenotype indicated a deficit in complex motor behavior (rotarod and coat hanger tests), rather than a decrease in locomotor and/or muscle strength (total activity and rearing in open field and EPM; early occurrence rather than accelerated frailty). This suggested a deficit in higher coordination, rather than a potential degeneration of spinal motor neurons, although a direct examination of the integrity of these neurons will be necessary to rule out this possibility. In the central nervous system, 5-HT<sub>1B</sub>R indirectly regulates DA release in STR.<sup>31</sup> No evidence of altered DA terminal density and area was identified in STR of old (and young) WT or KO mice (Figure 3), thus also excluding a structural downregulation of the DA system as the cause of the motor deficits in young *Htr1b*<sup>KO</sup> mice, although a role for altered DA kinetics in aging KO animals can not be ruled out. Moreover, the behavior decline could also be mediated through altered signaling at several other 5-HT receptors, due to altered 5-HT kinetics.<sup>27,31</sup> Thus, currently the exact mechanism leading to the motor phenotype is unknown, and may involve additional brain areas and systems not investigated here. Due to the complex biological nature of motor coordination and for the purpose of this study, we have considered the *Htr1b*<sup>KO</sup> motor phenotype as an indicator of changes in overall age-related functions, while we have

concentrated our molecular studies on FC and STR, as two brain areas with well-described roles for 5-HT<sub>1B</sub>R. Furthermore, investigating the FC allowed for the direct comparison of age-related molecular changes in WT and *Htr1b*<sup>KO</sup> mice with our prior characterization of aging in the human brain.<sup>36</sup> Eventually, studies using regional-, cell type- and time-specific targeted manipulations of 5-HT<sub>1B</sub>R in conditional mutant mice will be necessary to investigate the more specific roles of critical brain regions, time periods and interacting neurotransmitter systems that may participate in the different aspects of the behavioral and molecular phenotypes, and that underscore the increased vulnerability to age-related events in *Htr1b*<sup>KO</sup> mice.

In conclusion, our studies suggest a brain-driven age-related phenotype in mice lacking the presynaptic 5-HT<sub>1B</sub>R. The notion of altered longevity and early onset of age-dependent events due to changes in the brain represents an important novel finding, which is however not unprecedented. For instance, in lower eukaryotes, the well-characterized changes in longevity due to mutations in the IGF-1 pathway is rescued only when signal transduction is restored in neurons and not in other cell types of nematodes<sup>69</sup> and flies,<sup>70</sup> therefore providing supporting evidence for a control of age-related processes by the brain. Here, as the 'onset' rather than the 'nature' of aging was affected in *Htr1b*<sup>KO</sup> mice, 5-HT can be considered a modulator of 'normal' aging of the brain, consistently with its role in adapting to environmental challenges and maintaining homeostasis. As the 5-HT system is the target of chronic pharmacological interventions for psychiatric and other diseases, these results raise the possibility of long-term and/or age-related consequences to 5-HT manipulation that will need to be addressed in future studies. Pursuant is the potential for altered molecular and/or behavioral age-related trajectories in correlation with genetic polymorphisms in the *Htr1b* gene or other key regulators<sup>71</sup> of the 5-HT system.

## Acknowledgments

We thank Irwin Lucki and Anita Bechtholt for help with additional rodent support, Ruomei Liang for technical help, and David Lewis and Karoly Mirnics for helpful comments on the manuscript. This work was supported by NIMH (ES).

## References

- 1 Resnick SM, Pham DL, Kraut MA, Zonderman AB, Davatzikos C. Longitudinal magnetic resonance imaging studies of older adults: a shrinking brain. *J Neurosci* 2003; **23**: 3295–3301.
- 2 Sowell ER, Peterson BS, Thompson PM, Welcome SE, Henkenius AL, Toga AW. Mapping cortical change across the human life span. *Nat Neurosci* 2003; **6**: 309–315.
- 3 Terry RD, DeTeresa R, Hansen LA. Neocortical cell counts in normal human adult aging. *Ann Neurol* 1987; **21**: 530–539.

- 4 Bertoni-Freddari C, Fattoretti P, Paoloni R, Caselli U, Galeazzi L, Meier-Ruge W. Synaptic structural dynamics and aging. *Gerontology* 1996; **42**: 170–180.
- 5 Pakkenberg B, Gundersen HJ. Neocortical neuron number in humans: effect of sex and age. *J Comp Neurol* 1997; **384**: 312–320.
- 6 Park DC, Lautenschlager G, Hedden T, Davidson NS, Smith AD, Smith PK. Models of visuospatial and verbal memory across the adult life span. *Psychol Aging* 2002; **17**: 299–320.
- 7 Thibault O, Hadley R, Landfield PW. Elevated postsynaptic [Ca<sup>2+</sup>] and L-type calcium channel activity in aged hippocampal neurons: relationship to impaired synaptic plasticity. *J Neurosci* 2001; **21**: 9744–9756.
- 8 Davare MA, Hell JW. Increased phosphorylation of the neuronal L-type Ca<sup>2+</sup> channel Cav1.2 during aging. *Proc Natl Acad Sci USA* 2003; **100**: 16018–16023.
- 9 Verkhratsky A, Toescu EC. Calcium and neuronal ageing. *Trends Neurosci* 1998; **21**: 2–7.
- 10 Lerer B, Gillon D, Lichtenberg P, Gorfine M, Gelfin Y, Shapira B. Interrelationship of age, depression, and central serotonergic function: evidence from fenfluramine challenge studies. *Int Psychogeriatr* 1996; **8**: 83–102.
- 11 Mattson MP, Magnus T. Ageing and neuronal vulnerability. *Nat Rev Neurosci* 2006; **7**: 278–294.
- 12 Meltzer CC, Smith G, DeKosky ST, Pollock BG, Mathis CA, Moore RY *et al*. Serotonin in aging, late-life depression, and Alzheimer's disease: the emerging role of functional imaging. *Neuropsychopharmacology* 1998; **18**: 407–430.
- 13 Reynolds III CF, Kupfer DJ. Depression and aging: a look to the future. *Psychiatr Serv* 1999; **50**: 1167–1172.
- 14 Morrison JH, Hof PR. Life and death of neurons in the aging brain. *Science* 1997; **278**: 412–419.
- 15 Carlsson A. Neurotransmitter changes in the aging brain. *Dan Med Bull* 1985; **32**(Suppl 1): 40–43.
- 16 Davidoff MS, Lolova IS. Age-related changes in serotonin-immunoreactivity in the telencephalon and diencephalon of rats. *J Hirnforsch* 1991; **32**: 745–753.
- 17 Nishimura A, Ueda S, Takeuchi Y, Matsushita H, Sawada T, Kawata M. Vulnerability to aging in the rat serotonergic system. *Acta Neuropathol (Berlin)* 1998; **96**: 581–595.
- 18 Arango V, Ernberger P, Marzuk PM, Chen JS, Tierney H, Stanley M *et al*. Autoradiographic demonstration of increased serotonin 5-HT<sub>2</sub> and beta-adrenergic receptor binding sites in the brain of suicide victims. *Arch Gen Psychiatry* 1990; **47**: 1038–1047.
- 19 Marcusson J, Orelund L, Winblad B. Effect of age on human brain serotonin (S-1) binding sites. *J Neurochem* 1984; **43**: 1699–1705.
- 20 Marcusson JO, Morgan DG, Winblad B, Finch CE. Serotonin-2 binding sites in human frontal cortex and hippocampus. Selective loss of S-2A sites with age. *Brain Res* 1984; **311**: 51–56.
- 21 Bach-Mizrahi H, Underwood MD, Kassir SA, Bakalian MJ, Sibille E, Tamir H *et al*. Neuronal tryptophan hydroxylase mRNA expression in the human dorsal and median Raphe nuclei: major depression and suicide. *Neuropsychopharmacology* 2005; **31**: 814–824.
- 22 Meltzer CC, Smith G, Price JC, Reynolds III CF, Mathis CA, Greer P *et al*. Reduced binding of [<sup>18</sup>F]altanserin to serotonin type 2A receptors in aging: persistence of effect after partial volume correction. *Brain Res* 1998; **813**: 167–171.
- 23 Goldberg S, Smith GS, Barnes A, Ma Y, Kramer E, Robeson K *et al*. Serotonin modulation of cerebral glucose metabolism in normal aging. *Neurobiol Aging* 2004; **25**: 167–174.
- 24 van Luijckelaar MG, Tonnaer JA, Steinbusch HW. Aging of the serotonergic system in the rat forebrain: an immunocytochemical and neurochemical study. *Neurobiol Aging* 1992; **13**: 201–215.
- 25 Mattson MP, Maudsley S, Martin B. A neural signaling triumvirate that influences ageing and age-related disease: insulin/IGF-1, BDNF and serotonin. *Ageing Res Rev* 2004; **3**: 445–464.
- 26 David DJ, Bourin M, Hascoet M, Colombel MC, Baker GB, Jolliet P. Comparison of antidepressant activity in 4- and 40-week-old male mice in the forced swimming test: involvement of 5-HT<sub>1A</sub> and 5-HT<sub>1B</sub> receptors in old mice. *Psychopharmacology (Berlin)* 2001; **153**: 443–449.
- 27 Trillat AC, Malagie I, Scarce K, Pons D, Anmella MC, Jacquot C *et al*. Regulation of serotonin release in the frontal cortex and ventral hippocampus of homozygous mice lacking 5-HT<sub>1B</sub> receptors: *in vivo* microdialysis studies. *J Neurochem* 1997; **69**: 2019–2025.
- 28 Ramboz S, Saudou F, Amara DA, Belzung C, Dierich A, LeMeur M *et al*. Behavioral characterization of mice lacking the 5-HT<sub>1B</sub> receptor. *NIDA Res Monogr* 1996; **161**: 39–57.
- 29 Caspi A, Moffitt TE. Gene-environment interactions in psychiatry: joining forces with neuroscience. *Nat Rev Neurosci* 2006; **7**: 583–590.
- 30 Saudou F, Amara DA, Dierich A, LeMeur M, Ramboz S, Segu L *et al*. Enhanced aggressive behavior in mice lacking 5-HT<sub>1B</sub> receptor. *Science* 1994; **265**: 1875–1878.
- 31 Shippenberg TS, Hen R, He M. Region-specific enhancement of basal extracellular and cocaine-evoked dopamine levels following constitutive deletion of the serotonin(1B) receptor. *J Neurochem* 2000; **75**: 258–265.
- 32 Ase AR, Reader TA, Hen R, Riad M, Descarries L. Altered serotonin and dopamine metabolism in the CNS of serotonin 5-HT(1A) or 5-HT(1B) receptor knockout mice. *J Neurochem* 2000; **75**: 2415–2426.
- 33 Joyal CC, Beaudin S, Lalonde R. Longitudinal age-related changes in motor activities and spatial orientation in CD-1 mice. *Arch Physiol Biochem* 2000; **108**: 248–256.
- 34 Paxinos G, Franklin KBJ. *The Mouse Brain in Stereotaxic Coordinates*. Academic Press: San Diego, CA, 2001.
- 35 Irizarry RA, Bolstad BM, Collin F, Cope LM, Hobbs B, Speed TP. Summaries of Affymetrix GeneChip probe level data. *Nucleic Acids Res* 2003; **31**: e15.
- 36 Erraji-Benchekroun L, Underwood MD, Arango V, Galfalvy HC, Pavlidis P, Smyrniotopoulos P *et al*. Molecular aging in human prefrontal cortex is selective and continuous throughout adult life. *Biol Psychiatry* 2005; **57**: 549–558.
- 37 Glorioso C, Sabatini M, Unger T, Hashimoto T, Monteggia LM, Lewis DA *et al*. Specificity and timing of neocortical transcriptome changes in response to BDNF gene ablation during embryogenesis or adulthood. *Mol Psychiatry* 2006; **11**: 633–648.
- 38 Pavlidis P, Lewis DP, Noble WS. Exploring gene expression data with class scores. *Pac Symp Biocomput* 2002; **1**: 474–485.
- 39 Pavlidis P, Qin J, Arango V, Mann JJ, Sibille E. Using the Gene Ontology for microarray data mining: a comparison of methods and application to age effects in the human prefrontal cortex. *Neurochem Res* 2004; **29**: 1213–1222.
- 40 Ashburner M, Ball CA, Blake JA, Botstein D, Butler H, Cherry JM *et al*. Gene ontology: tool for the unification of biology. The Gene Ontology Consortium. *Nat Genet* 2000; **25**: 25–29.
- 41 Galfalvy HC, Erraji-Benchekroun L, Smyrniotopoulos P, Pavlidis P, Ellis SP, Mann JJ *et al*. Sex genes for genomic analysis in human brain: internal controls for comparison of probe level data extraction. *BMC Bioinformatics* 2003; **4**: 37.
- 42 Sibille E, Hen R. Serotonin(1A) receptors in mood disorders: a combined genetic and genomic approach. *Behav Pharmacol* 2001; **12**: 429–438.
- 43 Hashimoto T, Volk DW, Eggan SM, Mirnics K, Pierri JN, Sun Z *et al*. Gene expression deficits in a subclass of GABA neurons in the prefrontal cortex of subjects with schizophrenia. *J Neurosci* 2003; **23**: 6315–6326.
- 44 Buhot MC, Wolff M, Benhassine N, Costet P, Hen R, Segu L. Spatial learning in the 5-HT<sub>1B</sub> receptor knockout mouse: selective facilitation/impairment depending on the cognitive demand. *Learn Mem* 2003; **10**: 466–477.
- 45 Keegan A, Morecroft I, Smillie D, Hicks MN, MacLean MR. Contribution of the 5-HT(1B) receptor to hypoxia-induced pulmonary hypertension: converging evidence using 5-HT(1B)-receptor knockout mice and the 5-HT(1B/1D)-receptor antagonist GR127935. *Circ Res* 2001; **89**: 1231–1239.
- 46 Ciaranello RD, Tan GL, Dean R. G-protein-linked serotonin receptors in mouse kidney exhibit identical properties to 5-HT<sub>1b</sub> receptors in brain. *J Pharmacol Exp Ther* 1990; **252**: 1347–1354.
- 47 Gershon MD. Review article: serotonin receptors and transporters – roles in normal and abnormal gastrointestinal motility. *Aliment Pharmacol Ther* 2004; **20**(Suppl 7): 3–14.
- 48 Mossner R, Lesch KP. Role of serotonin in the immune system and in neuroimmune interactions. *Brain Behav Immun* 1998; **12**: 249–271.
- 49 Tatar M, Bartke A, Antebi A. The endocrine regulation of aging by insulin-like signals. *Science* 2003; **299**: 1346–1351.
- 50 Suji G, Sivakami S. Glucose, glycation and aging. *Biogerontology* 2004; **5**: 365–373.

- 51 Holzenberger M, Dupont J, Ducos B, Leneuve P, Geloën A, Even PC *et al*. IGF-1 receptor regulates lifespan and resistance to oxidative stress in mice. *Nature* 2003; **421**: 182–187.
- 52 Lee CK, Weindruch R, Prolla TA. Gene-expression profile of the ageing brain in mice. *Nat Genet* 2000; **25**: 294–297.
- 53 Lu T, Pan Y, Kao SY, Li C, Kohane I, Chan J *et al*. Gene regulation and DNA damage in the ageing human brain. *Nature* 2004; **429**: 883–891.
- 54 DeVellis JS. *Neuroglia in the Aging Brain*. Humana Press: Totowa, NJ, 2002.
- 55 Webster MJ, Weickert CS, Herman MM, Kleinman JE. BDNF mRNA expression during postnatal development, maturation and aging of the human prefrontal cortex. *Brain Res Dev Brain Res* 2002; **139**: 139–150.
- 56 Hekimi S, Guarente L. Genetics and the specificity of the aging process. *Science* 2003; **299**: 1351–1354.
- 57 Fabrizio P, Gattazzo C, Battistella L, Wei M, Cheng C, McGrew K *et al*. Sir2 blocks extreme life-span extension. *Cell* 2005; **123**: 655–667.
- 58 Parker JA, Arango M, Abderrahmane S, Lambert E, Tourette C, Catoire H *et al*. Resveratrol rescues mutant polyglutamine cytotoxicity in nematode and mammalian neurons. *Nat Genet* 2005; **37**: 349–350.
- 59 Caspi A, Sugden K, Moffitt TE, Taylor A, Craig IW, Harrington H *et al*. Influence of life stress on depression: moderation by a polymorphism in the 5-HTT gene. *Science* 2003; **301**: 386–389.
- 60 Kujoth GC, Hiona A, Pugh TD, Someya S, Panzer K, Wohlgemuth SE *et al*. Mitochondrial DNA mutations, oxidative stress, and apoptosis in mammalian aging. *Science* 2005; **309**: 481–484.
- 61 Kuro-o M, Matsumura Y, Aizawa H, Kawaguchi H, Suga T, Utsugi T *et al*. Mutation of the mouse *klotho* gene leads to a syndrome resembling ageing. *Nature* 1997; **390**: 45–51.
- 62 Mounkes LC, Kozlov S, Hernandez L, Sullivan T, Stewart CL. A progeroid syndrome in mice is caused by defects in A-type lamins. *Nature* 2003; **423**: 298–301.
- 63 Trifunovic A, Wredenberg A, Falkenberg M, Spelbrink JN, Rovio AT, Bruder CE *et al*. Premature ageing in mice expressing defective mitochondrial DNA polymerase. *Nature* 2004; **429**: 417–423.
- 64 Finch CE. Neurons, glia, and plasticity in normal brain aging. *Adv Gerontol* 2002; **10**: 35–39.
- 65 Malberg JE, Eisch AJ, Nestler EJ, Duman RS. Chronic antidepressant treatment increases neurogenesis in adult rat hippocampus. *J Neurosci* 2000; **20**: 9104–9110.
- 66 Niedernhofer LJ, Garinis GA, Raams A, Lalai AS, Robinson AR, Appeldoorn E *et al*. A new progeroid syndrome reveals that genotoxic stress suppresses the somatotroph axis. *Nature* 2006; **444**: 1038–1043.
- 67 Alvarez FJ, Pearson JC, Harrington D, Dewey D, Torbeck L, Fyffe RE. Distribution of 5-hydroxytryptamine-immunoreactive boutons on alpha-motoneurons in the lumbar spinal cord of adult cats. *J Comp Neurol* 1998; **393**: 69–83.
- 68 Wallis DI. 5-HT receptors involved in initiation or modulation of motor patterns: opportunities for drug development. *Trends Pharmacol Sci* 1994; **15**: 288–292.
- 69 Wolkow CA, Kimura KD, Lee MS, Ruvkun G. Regulation of *C. elegans* life-span by insulin like signaling in the nervous system. *Science* 2000; **290**: 147–150.
- 70 Hwangbo DS, Gershman B, Tu MP, Palmer M, Tatar M. Drosophila dFOXO controls lifespan and regulates insulin signalling in brain and fat body. *Nature* 2004; **429**: 562–566.
- 71 Payton A, Gibbons L, Davidson Y, Ollier W, Rabbitt P, Worthington J *et al*. Influence of serotonin transporter gene polymorphisms on cognitive decline and cognitive abilities in a nondemented elderly population. *Mol Psychiatry* 2005; **10**: 1133–1139.

Supplementary Information accompanies the paper on the Molecular Psychiatry website (<http://www.nature.com/mp>)